

# Spin multistability of cavity polaritons in a magnetic field

S. S. Gavrilov,<sup>1,\*</sup> A. V. Sekretenko,<sup>1</sup> N. A. Gippius,<sup>2,3</sup> C. Schneider,<sup>4</sup>  
S. Höfling,<sup>4</sup> M. Kamp,<sup>4</sup> A. Forchel,<sup>4</sup> and V. D. Kulakovskii<sup>1</sup>

<sup>1</sup>*Institute of Solid State Physics RAS, Chernogolovka, 142432, Russia*

<sup>2</sup>*A. M. Prokhorov General Physics Institute, RAS, Moscow 119991, Russia*

<sup>3</sup>*LASMEA, UMR 6602 CNRS, Université Blaise Pascal, 63177 Aubière, France*

<sup>4</sup>*Technische Physik, Physikalisches Institut and Wilhelm Conrad Röntgen Research Center for Complex Material Systems, Universität Würzburg, D-97074 Würzburg, Germany*

(Dated: July 6, 2018)

Spin transitions are studied theoretically and experimentally in a resonantly excited system of cavity polaritons in a magnetic field. Weak pair interactions in this boson system make possible fast and massive spin flips occurring at critical amplitudes due to the interplay between amplitude dependent shifts of eigenstates and the Zeeman splitting. Dominant spin of a condensate can be toggled forth and back by tuning of the pump intensity only, which opens the way for ultra-fast spin switchings of polariton condensates on a picosecond timescale.

PACS numbers: 71.36.+c, 42.65.Pc

Collective phenomena in cavity-polariton systems attract a broad interest during the last decade. Being weakly interacting bosons formed due to strong exciton-photon coupling in microcavities [1], polaritons exhibit collective properties typical of both matter waves and light waves, including optic parametric scattering [2] and Bose condensation [3]. The combination of non-zero spin, spin-sensitive interactions and the ability of polaritons to form macro-occupied states allows studying a row of new spin phenomena manifesting themselves in the transitions between distinct spin states of multi-component condensates. Cavity-polariton systems are much more convenient to explore by optical means than condensates in He-3 or other Bose systems with non-zero spin those, however, may exhibit similar collective properties due to spin-dependent interactions.

Under resonant excitation, polariton-polariton interactions lead to a multistable behavior of polariton condensates with several steady states feasible at fixed pump parameters [4–14]. A switching between the steady-state branches nearby bifurcation points is accompanied by sharp jumps in the cavity-field intensity and polarization. The state of the spin-up or spin-down component of the condensate is switched due to a feedback loop between its amplitude and effective resonance frequency. The same kind of transitions is also responsible for many-mode optical parametric oscillation [15, 16], spin ring patterns [5, 9–11], and bright polariton solitons [17], which all would be impossible without polariton bi- or multistability. The energy-shifting interactions are also known to cause spin transitions in non-resonantly pumped polariton condensates in a magnetic field [18, 19].

By now, many-branch multistability of polariton condensates has been evidenced under continuous-wave (cw) excitation in few  $\mu\text{m}$  wide cavity mesas [8]. It was shown that the average spin of the condensate can be triggered

from almost  $-1$  to  $+1$  by varying the degree of circular polarization of the pump wave within a comparatively narrow interval. However, changing the pump intensity at a fixed pump polarization cannot alter the dominant spin of the condensate that, in this case, is pinned to dominantly right or left polarization of the pump wave. The necessity to tune the input polarization leaves open the question on how fast such spin inversions of condensates can be, since a controllable tuning of light polarization on a picosecond timescale (that is comparable to the lifetime of cavity polaritons) is quite problematic.

In this Letter we study transitions between distinct spin states of many-polariton systems resonantly excited in a planar cavity placed into a magnetic field. The condensates are shown to have coexistent opposite-spin states in a wide range of pump powers and polarizations. We found that the interplay between blue-shifts of eigenstates and the Zeeman effect releases the spin pinning, so that a condensate can be switched between opposite-spin states by varying the intensity even keeping fixed the polarization of the pump wave. As such, it constitutes a qualitatively new kind of multistability that enables spin-inverting transitions of multi-component bosonic condensates within extremely short time intervals under pulsed photoexcitation. We have tracked the cavity transmission under 100 ps pump pulses and found the time of the transition between opposite-spin states of a polariton condensate to be about ten picoseconds.

*Multistability and steady-state solutions.*—Resonantly driven cavity-polariton condensates are usually considered within a coherent mean-field approach based on the Gross-Pitaevskii equations. For simplicity we write them for the single lower polariton mode driven by a coherent

pump with zero in-plane wave vector ( $\mathbf{k} = 0$ ) [4–7, 19]:

$$i\hbar \frac{d}{dt} \begin{pmatrix} \psi_+ \\ \psi_- \end{pmatrix} = \begin{pmatrix} \hat{E}_0 - i\hat{\gamma}_0 \end{pmatrix} \begin{pmatrix} \psi_+ \\ \psi_- \end{pmatrix} + \begin{pmatrix} (V_1|\psi_+|^2 + V_2|\psi_-|^2)\psi_+ \\ (V_2|\psi_+|^2 + V_1|\psi_-|^2)\psi_- \end{pmatrix} + \begin{pmatrix} F_+(t) \\ F_-(t) \end{pmatrix}. \quad (1)$$

Herein are  $F_{\pm}(t) = \sqrt{\frac{I_p(t)}{2}}(1 \pm \rho_p)e^{i(E_p/\hbar)t + i\phi_{\pm}}$ ;  $I_p = |F_+|^2 + |F_-|^2$  the pump intensity,  $\rho_p$  the degree of circular polarization,  $E_p$  the pump energy, and  $\Phi_p = \phi_+ - \phi_-$  the phase shift between the  $\sigma^{\pm}$  components of the pump wave.  $V_{1,2}$  are the polariton-polariton interaction constants. The polariton mode is characterized by its energy  $\hat{E}_0$  and decay rate  $\hat{\gamma}_0$  which are  $2 \times 2$  matrices written in the  $\sigma^{\pm}$  basis. For simplicity we assume  $\hat{\gamma}_0$  to be spin-symmetric,  $\hat{\gamma}_0 = \gamma_0 \hat{1}$ , whereas  $\hat{E}_0$  has the form

$$\hat{E}_0 = E_0 \hat{1} + \frac{\delta_c}{2} \begin{pmatrix} 1 & 0 \\ 0 & -1 \end{pmatrix} + \frac{\delta_l}{2} \begin{pmatrix} 0 & 1 \\ 1 & 0 \end{pmatrix}. \quad (2)$$

Its first term is the energy of polaritons in a symmetric structure, the second term provides the  $\sigma^{\pm}$  splitting,  $E_0^+ - E_0^- = \delta_c$ , and the third term gives the X-Y splitting  $E_0^{(x)} - E_0^{(y)} = \delta_l$  in the Cartesian basis  $\begin{pmatrix} \psi_x \\ \psi_y \end{pmatrix} = \frac{1}{\sqrt{2}} \begin{pmatrix} 1 & 1 \\ i & -i \end{pmatrix} \begin{pmatrix} \psi_+ \\ \psi_- \end{pmatrix}$ . The X-Y splitting may be due to crystalline disorder or TE-TM splitting of cavity photons at  $\mathbf{k} \neq 0$ .

The interaction between polaritons with anti-parallel spins ( $V_2$ ) is attractive and typically much weaker than that between polaritons with parallel spins ( $V_1$ ) [20–22]; below we assume  $V_2 = -0.1V_1$ . The units for  $\psi$  can be fixed by the condition  $V_1 = 1$ , so that  $|\psi|^2$  has the dimension of energy and, in the case of circularly polarized excitation, coincides with the blue-shift of the driven mode. In the following simulations we set  $\gamma_0 = 0.05$  meV and  $\Delta = E_p - E_0 = 0.2$  meV.

By substituting  $\psi_{\pm}(t) = \tilde{\psi}_{\pm}e^{-i(E_p/\hbar)t}$  into Eq. (1) one gets a time-independent equation that allows one to find the response of the driven condensate mode on a constant pump,  $\tilde{\psi}_{\pm} = \tilde{\psi}_{\pm}(I_p, \rho_p, \Phi_p)$ . The problem concerned with asymptotic stability of the steady-state solutions was considered in Ref. [7].

In the simplest case of a degenerate system ( $\delta_{c,l} = 0$ ) under purely circular excitation ( $\rho_p = 1$ ), the dependence of the steady-state cavity-field intensity on pump intensity takes the form of an ‘S’-shaped circuit [23, 24] (Fig. 1a). This implies, first, the possibility of a jump (“switch-up”) in the cavity transmission and, second, the hysteresis of the response under slowly changing pump power. As long as  $|V_2| \ll V_1$ , the response of the system excited with elliptically polarized light may be treated in terms of the two S-circuits corresponding to (almost uncoupled)  $\sigma^+$  and  $\sigma^-$  polarization components. A growth of pump density involves two successive switch-ups, in the dominant  $\sigma^+$  or  $\sigma^-$  condensate component and then in the minor one [4, 5] (Fig. 1b).

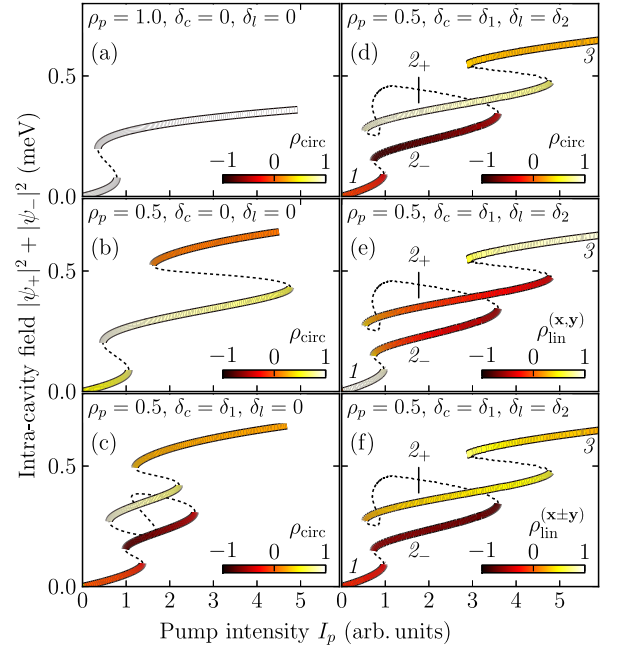


FIG. 1. (Color online) The steady-state response of the driven polariton mode,  $|\psi_+|^2 + |\psi_-|^2$  vs.  $I_p$ , for several combinations of  $\rho_p$ ,  $\delta_c$ , and  $\delta_l$  which are indicated at the top of each panel ( $\delta_1 = -0.12$  meV,  $\delta_2 = 0.05$  meV,  $\Phi_p = 0$ ). The branches of asymptotically stable solutions are shown by colored heavy lines, the color indicates the degrees of circular polarization (a–d) and linear polarization in  $(\mathbf{x}, \mathbf{y})$  basis (e) and  $(\mathbf{x}+\mathbf{y}, \mathbf{x}-\mathbf{y})$  basis (f); unstable branches are shown by dashed lines.

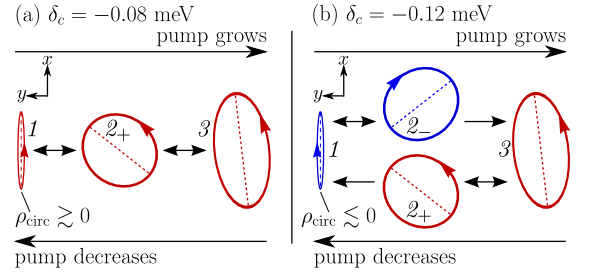


FIG. 2. (Color online) The scheme of non-equilibrium transitions at (a)  $\delta_c = -0.08$  meV and (b)  $\delta_c = -0.12$  meV; in both cases  $\delta_l = 0.05$  meV,  $\rho_p = 0.5$ ,  $\Phi_p = 0$ . Ellipses schematically represent the polarizations typical of the stability branches 1,  $2_{\pm}$ , and 3 which are explicitly labeled in Fig. 1d–f.

In a magnetic field the response diagram becomes qualitatively different if  $\rho_p$  and  $\delta_c = E_0^+ - E_0^-$  have opposite signs, i. e. if the pump polarization is biased towards that of the lower split-off polariton level. In this case each of the  $\sigma^{\pm}$  modes has its own advantage over the other: whilst the lower one is pumped more “intensively” (e. g.  $|F_+| > |F_-|$ ), the upper one is closer to the resonance with the pump field that is blue-detuned from both. As a result, for a certain pump there may coexist three high-energy branches corresponding to spin-up and spin-down components switched-up individually and in combination

(Fig. 1c). Due to the same reason the circular polarization in the lowermost state can be either positive (right) or negative (left) depending on  $\Delta$  and  $\delta_{c,l}$ .

Fig. 1d represents the system with  $\rho_p = +0.5$ ,  $\delta_c = E_0^+ - E_0^- = -0.12$  meV, and  $\delta_l = E_0^{(x)} - E_0^{(y)} = 0.05$  meV; the main axis of pump polarization is  $x$ -directed, so that  $\Phi_p = 0$ . The X-Y splitting involves the mixing of the  $\sigma^\pm$  polarization components, which is sensitive to the phase difference of  $\psi_\pm$  [8, 13]. In the considered case it extends the range of  $I_p$  where only one of the  $\sigma^\pm$  components is found in the “up” position. If the sign of  $\delta_l$  were negative (or the pump polarization were  $y$ -directed), the region with the two highly polarized stability branches would be reduced [14].

*Transitions between stability branches.* In a degenerate system the order of the switch-ups is rigidly determined by the bias of pump polarization; the reverse transitions observed in the course of decreasing pump always proceed in the “last-up, first-down” order (Fig. 1b). In a magnetic field, such a behavior takes place at small  $\delta_c$  (Fig. 2a), but at larger  $\delta_c$  a new evolution scenario appears (Fig. 2b). Given the system starts from the lower stability branch (1) in Fig. 1d, a slowly increasing pump successively transfers it to branch  $2_-$  (that is mainly  $\sigma^-$  polarized) and then to branch 3 [?]. However, the reverse transition  $3 \rightarrow 1$  proceeds through the  $\sigma^+$ -polarized branch  $2_+$ . Thus, the transitions occur in the “last-up, last-down” order that allows the cavity-field polarization to be inverted. It constitutes a qualitatively distinct type of multistability from that in spin-degenerate polariton systems [4, 5, 7–10].

As shown by numerical simulations performed for 70 ps long pump pulses (see below), the system undergoes either  $1 \rightarrow 2_+$  or  $1 \rightarrow 2_-$  transformation depending on the sign of polarization ( $\rho_{\text{circ}}$ ) in the low-energy state at branch 1 (Fig. 2). In other words, a small externally controlled right or left bias of *intra-cavity* rather than external (pump) polarization determines the branch the system comes to on reaching the threshold pump power.

*Experiment.*—The sample has four 7 nm thick GaAs quantum wells separated by 4 nm AlAs barriers which are centered in a half- $\lambda$  cavity. Its top (bottom) mirror consists of 32 (36)  $\text{Al}_{0.2}\text{Ga}_{0.8}\text{As}/\text{AlAs}$  Bragg reflectors; GaAs substrate was etched in order to perform transmission measurements. The  $Q$ -factor is  $7 \cdot 10^3$ ; the Rabi splitting and the exciton-photon detuning are 10.5 meV and  $E_C - E_X(\mathbf{k}=0) \approx -5$  meV, respectively; the decay rate of the lower polariton state at  $\mathbf{k}=0$  is  $\gamma_0 \approx 0.05$  meV. The sample, placed into the magneto-optical cryostat at  $T = 2$  K, is excited by optic pulses with a repetition rate of 8 MHz and duration of 70 ps generated by a mode-locked Ti:sapphire laser. The pump beam is directed along the cavity normal and focused into a  $30 \mu\text{m}$  wide spot on the sample. The transmission signal is detected by a streak-camera with spatial and time resolutions of

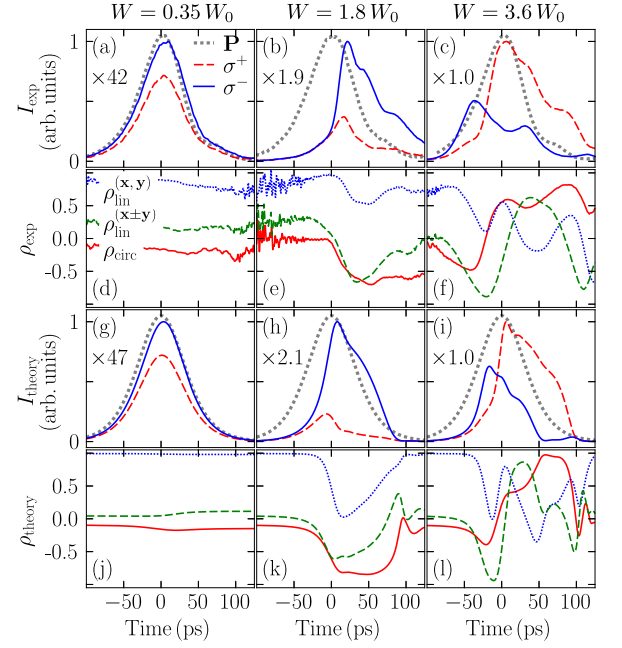


FIG. 3. (Color online) (a–c) Measured time dependences of the  $\sigma^+$  (solid lines) and  $\sigma^-$  (dashed lines) components of the transmission signal at  $\delta_c = -0.12$  meV; the pump shape is shown by heavy dotted lines. (d–f) The corresponding time dependences of the signal polarization in the circular basis (solid lines),  $(x, y)$  basis (dotted lines), and  $(x \pm y)$  basis (dashed lines). Different columns correspond to different peak pump powers indicated at the top panels. (g–l) The modeled counterpart time dependences.

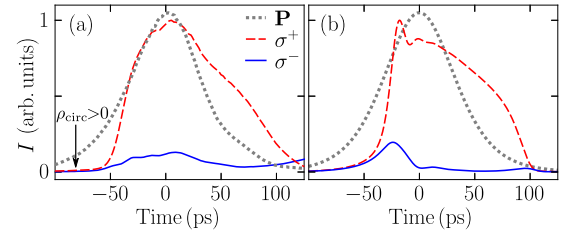


FIG. 4. (a) Measured and (b) calculated time dependences of the  $\sigma^+$  and  $\sigma^-$  components of the transmission signal at  $\delta_c = -0.08$  meV and  $W = 3.6 W_0$ .

$7 \mu\text{m}$  and 6 ps, respectively. Under a weak excitation in a zero magnetic field the cavity spectrum exhibits two linearly polarized levels separated by  $\delta_l \approx 0.05$  meV.

To perform simulations, we solve numerically the many-mode Gross-Pitaevskii equations of type (1) [7] with a  $30 \mu\text{m}$  wide Gaussian pump source; the model parameters nearly coincide with the experimental ones. In order to avoid complexity brought on by spatial inhomogeneity of the transmission (see [5, 9, 10]), below we only consider the time dependences of the signal collected from the spot center (in both the experiment and modeling). At last, in order to simulate finite time resolution and a partial weakly controlled time and space smooth-

ing of the measured signal, the calculated intensities are averaged over the neighboring 10 ps in each time point.

Fig. 3 shows the dynamics of the system whose steady-state properties have been discussed in Figs. 1d–f. Most importantly, the pump polarization is biased towards the lower split-off circular polarization component ( $\rho_p = +0.5$ ) and the upper linearly polarized eigenstate of a spin-degenerate system (the  $x$  direction). The Zeeman splitting  $\delta_c \approx -0.12$  meV is involved by the magnetic field  $B \approx 6$  T. The three basis polarization degrees of the signal, the circular one,  $\rho_{\text{circ}}$ , and two linear ones,  $\rho_{\text{lin}}^{(\mathbf{x},\mathbf{y})}$  and  $\rho_{\text{lin}}^{(\mathbf{x}\pm\mathbf{y})}$ , are shown in Figs. 3d–f, whereas Figs. 3a–c show only the circularly polarized components of the transmission intensity. Left column in Fig. 3 represents the case of a low peak pump intensity  $W = \max_t I_p(t) \approx 0.35W_0$ , where  $W_0$  corresponds to the first switch-up point in both the experiment and calculation; in the experiment,  $W_0 \approx 500$  kW/cm<sup>2</sup>. In this case the signal polarization is nearly constant, though it does not coincide with that of the pump beam due to the splitting of polariton modes with different polarizations. In fact, the signal is almost linearly polarized with a slight bias towards  $\sigma^-$  according to Figs. 1d–f.

The middle column in Fig. 3 represents the above-threshold dynamics at  $W = 1.8W_0$ ; a 5-fold increase in  $W$  involves more than a 20-fold increase in the transmission signal (compare Figs. 3a,b). The signal appears to be mainly  $\sigma^-$ -polarized, and nearby the peak excitation it also exhibits a prominent polarization in the “diagonal” ( $\mathbf{x} - \mathbf{y}$ ) direction (see Fig. 3e). This makes up a clear manifestation of the  $1 \rightarrow 2_-$  transition (Fig. 1f).

A further two-fold increase in  $W$  up to  $3.6W_0$  (right column in Fig. 3) allows us to track the double  $1 \rightarrow 2_- \rightarrow 3$  transition proceeding during the growth of pump density as well as the “asymmetric” reverse transition  $3 \rightarrow 2_+$  at the back front of the pulse, which are schematically shown in Fig. 2b. In particular, according to Fig. 3c the signal exhibits first the switch-up in the  $\sigma^-$  component (leading to high negative values of  $\rho_{\text{circ}}$ ) and next, with increasing pump, the switch-up in  $\sigma^+$  (so that  $\rho_{\text{circ}}$  becomes positive). Finally, the switch-down in  $\sigma^-$  at the back front results in a further growth of  $\rho_{\text{circ}}$  up to values exceeding the pump polarization. The transitions observed in all the three basis polarizations agree with the simulation shown in Fig. 3i,l and conform to the steady-state diagram in Fig. 1d–f. According to the latter, (i)  $\rho_{\text{lin}}^{(\mathbf{x}\pm\mathbf{y})}(t)$  exhibits the sign reversal during the  $2_- \rightarrow 3$  transition and (ii)  $\rho_{\text{lin}}^{(\mathbf{x},\mathbf{y})}(t)$  has two minima, of which the first is immediately before the  $2_- \rightarrow 3$  transition ( $t \approx -20$  ps) and the second is immediately after the  $3 \rightarrow 2_+$  transition ( $t \approx +50$  ps).

The discussed transitions differ from those in a system with small  $\delta_c$  splitting. A typical dynamics in a 1.5 times smaller magnetic field ( $B = 4$  T, so that  $\delta_c = -0.08$  meV, and  $W = 3.6W_0$ ) is presented in Fig. 4. Its main dis-

tinguishing is a positive sign of the signal polarization in a low-energy state ( $\rho_{\text{circ}} > 0$  at  $t < -60$  ps), which predetermines the  $1 \rightarrow 2_+$  trajectory under increasing pump power. A further increase in  $W$  (not shown) involves the  $2_+ \rightarrow 3$  transition. In fact, this scenario, representing a steady-state scheme in Fig. 2a, is qualitatively the same as that predicted [4] and observed [9] for a spin-degenerate system. However, our system is not affected by the long-lived excitonic reservoir (see Refs. [9, 11, 25, 26]) due to a comparatively short duration of pump pulses.

To summarize, we have discovered a mechanism of ultra-fast spin flips in cavity-polariton condensates, which can be implemented in Bose systems with energy-split eigenstates of opposite spins. It is involved by amplitude dependent shifts of eigenstates due to spin-dependent inter-particle interactions. This effect can be used in the future highly tunable optic switchers and logic elements working in the picosecond range or for creating short light pulses with rapidly changing polarization.

The authors are grateful to V.B. Timofeev and S.G. Tikhodeev for fruitful discussions. This work was supported by the RF President grant MK-6863.2012.2, RFBR, and the State of Bavaria.

---

\* gavr\_ss@issp.ac.ru

- [1] C. Weisbuch *et al.*, Phys. Rev. Lett. **69**, 3314 (1992).
- [2] R. M. Stevenson *et al.*, Phys. Rev. Lett. **85**, 3680 (2000).
- [3] J. Kasprzak *et al.*, Nature **443**, 409414 (2006).
- [4] N. A. Gippius *et al.*, Phys. Rev. Lett. **98**, 236401 (2007).
- [5] I. A. Shelykh, T. C. H. Liew, and A. V. Kavokin, Phys. Rev. Lett. **100**, 116401 (2008).
- [6] T. C. H. Liew, A. V. Kavokin, and I. A. Shelykh, Phys. Rev. Lett. **101**, 016402 (2008).
- [7] S. S. Gavrilov *et al.*, JETP **110**, 825 (2010).
- [8] T. K. Paraïso *et al.*, Nat Mater **9**, 655 (2010).
- [9] D. Sarkar *et al.*, Phys. Rev. Lett. **105**, 216402 (2010).
- [10] C. Adrados *et al.*, Phys. Rev. Lett. **105**, 216403 (2010).
- [11] S. S. Gavrilov *et al.*, Phys. Rev. B **85**, 075319 (2012).
- [12] S. S. Gavrilov and N. A. Gippius, Phys. Rev. B **86**, 085317 (2012).
- [13] Ö. Bozat, I. G. Savenko, and I. A. Shelykh, Phys. Rev. B **86**, 035413 (2012).
- [14] S. S. Gavrilov *et al.*, APL **102**, 011104 (2013).
- [15] D. N. Krizhanovskii *et al.*, Phys. Rev. B **77**, 115336 (2008).
- [16] A. A. Demenev *et al.*, Phys. Rev. Lett. **101**, 136401 (2008).
- [17] M. Sich *et al.*, Nat Photon **6**, 5055 (2012).
- [18] A. V. Larionov *et al.*, Phys. Rev. Lett. **105**, 256401 (2010).
- [19] P. Walker *et al.*, Phys. Rev. Lett. **106**, 257401 (2011).
- [20] P. Renucci *et al.*, Phys. Rev. B **72**, 075317 (2005).
- [21] K. V. Kavokin *et al.*, Phys. Stat. Sol. (c) **2** (2005).
- [22] M. Vladimirova *et al.*, Phys. Rev. B **82**, 075301 (2010).
- [23] A. Baas *et al.*, Phys. Rev. A **69**, 023809 (2004).
- [24] N. A. Gippius *et al.*, EPL **67**, 997 (2004).

- [25] S. S. Gavrilov *et al.*, JETP Lett. **92**, 171 (2010).
- [26] D. V. Vishnevsky *et al.*, Phys. Rev. B **85**, 155328 (2012).